Bioorganic Chemistry 138 (2023) 106659

Contents lists available at ScienceDirect

Bioorganic Chemistry

journal homepage: www.elsevier.com/locate/bioorg

Synthesis and antitubercular activity of novel 4-arylalkyl substituted thio-, oxy- and sulfoxy-quinoline analogues targeting the cytochrome *bc*1 complex

Robert Murnane [a], Mire Zloh [b,c], Sangeeta Tanna [a], Renee Allen [d], Felipe Santana-Gomez [d], Tanya Parish [d], Federico Brucoli [a,*]

[a] Leicester School of Pharmacy, De Montfort University, Leicester LE1 9BH, UK
[b] Faculty of Pharmacy, University Business Academy, Novi Sad 2100, Serbia
[c] UCL School of Pharmacy, UCL, London WC1N 1AX, UK
[d] Center for Global Infectious Disease Research, Seattle Children's Research Institute, 307 Westlake Avenue North, Suite 500, Seattle, USA

ARTICLE INFO

Keywords:
Anti-microbial resistance
Quinoline
Tuberculosis
Oxidative phosphorylation
Bc1-aa3 super complex
QcrB mutants

ABSTRACT

A library of 4-substituted quinolines was synthesised based on the structural features of the privileged 4-(benzylthio)-6-methoxy-2-methylquinoline scaffold. Quinoline-based chemical probes have proven to be effective anti-tuberculosis agents with the ability of inhibiting components of *Mycobacterium tuberculosis* (MTB) respiratory chain including the *b* subunit of the cytochrome bc_1 complex. Novel 4-(arylalkyl)-thio, -oxy and sulfoxyquinoline analogues were tested for their ability to inhibit the growth of MTB H37Rv and QcrB mutant strains, and the compounds mode of action was investigated. Members of the 4-subtituted thio- and sulfoxyquinoline series exhibited significant growth inhibitory activity in the high nanomolar range against wild-type MTB and induced depletion of intracellular ATP. These probes also showed reduced potency in the QcrB T313I mutant strain, thus indicating the cytochrome bc_1 oxidase complex as the molecular target. Interestingly, new 4-(quinolin-2-yl)oxy-quinoline **4*i*** was more selective for the QcrB T313I strain compared to the wild-type strain.

1. Introduction

Tuberculosis (TB) is an ancient infectious disease caused by *Mycobacterium tuberculosis* that remains a threat to global health. In 2021, TB killed 1.6 million people and an estimated 10.6 million people contracted this disease worldwide, although there was a significant reduction in reported cases (from 7.1 million to 5.8 million) between 2019 and 2020 due to disruptions caused by the COVID-19 pandemic on TB services including cases notifications [1]. Notably, the TB incidence rate increased by 3.6% between 2020 and 2021 inverting the 2% yearly decline observed in the past two decades [1]. Most cases were in the WHO regions of South-East Asia (43%) and Africa (25%), and Western Pacific (18%), with lower percentages in Europe (2.3%). Amongst the top 30 high TB burden countries, eight accounted for the total number of cases worldwide, e.g., India, China, Indonesia, the Philippines, Pakistan, Nigeria, Bangladesh and South Africa [1]. However, TB is also a healthcare challenge in Europe, where 230,000 new cases with an estimated 20,000 deaths were reported in 2021. Further, an estimated 73,000 new cases of rifampicin-resistant and multidrug-resistant TB (RR/MDR TB) were reported in 2021 [1]. This is about 16% of the 450,000 RR/MDR TB cases worldwide in 2021 and Europe has the highest MDR TB rates in the world (SURVEILLANCE REPORT. Tuberculosis surveillance and monitoring in Europe 2018 (europa.eu)).

During the COVID-19 pandemic in 2020, TB was the second leading cause of death by infectious disease after COVID-19, and the annual number of estimated global TB deaths increased by 7.45% for the first time since 2005 from a previous year (*i.e.*, from 1.2 million in 2020 to 1.3 million in 2021) [1]. This spike in TB deaths was linked to the restrictions put in place during the COVID-19 pandemic, which hamstrung the services required to fight TB due to lack of funding and focus, distribution of essential treatments and delays in initial diagnosis. Notwithstanding the COVID-19 pandemic, the progress made against the goals laid out in 2014 by the World Health Assembly has been very disappointing, as incident and mortality rates were expected to be reduced by a minimum of 20% and 35% respectively from the initial 2015 rates by 2021. However, both rates fell by only a fraction of the

* Corresponding author.
E-mail address: federico.brucoli@dmu.ac.uk (F. Brucoli).

https://doi.org/10.1016/j.bioorg.2023.106659
Received 27 March 2023; Received in revised form 19 May 2023; Accepted 5 June 2023
Available online 7 June 2023

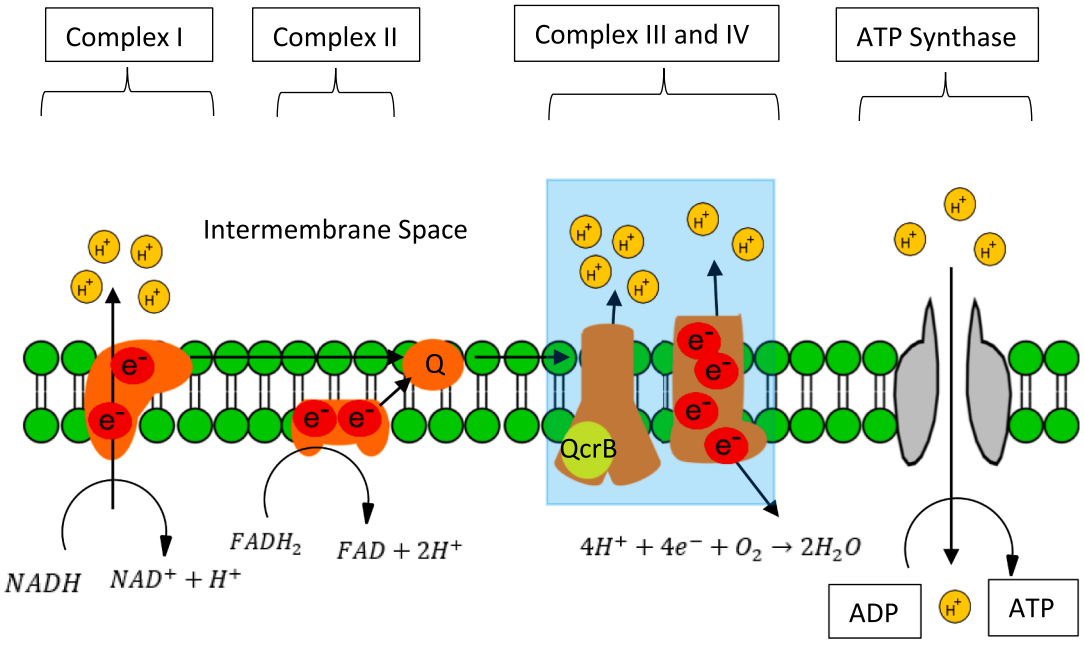

Fig. 1. Schematic representation of the electron transport chain in *M. tuberculosis*. The chain includes **Complexes I – IV** and **ATP synthase**. **Complex I** (NADH dehydrogenase) oxidizes NADH to NAD^+, allowing protons to cross from the cytoplasm to the intermembrane space. **Complex II** (coenzyme Q, or CoQ) receives electrons from Complex I, using $FADH_2$ as the electron source, and passes them onto **Complex III**, which contains cytochrome bc_1. Cytochrome bc_1, which includes the QcrB peptide, undergoes oxidation as the electrons are passed down the chain. For every two electrons transferred, four protons are translocated across the membrane. **Complex IV** (cytochrome aa_3) undergoes the same oxidization and reduction processes, as the electrons continue to be transferred through the chain. The electron transport chain is linked to ATP regeneration from ADP and the translocation of protons throughout the process creates a disparity in proton concentration between the cytoplasm and the intermembrane space. This imbalance creates a proton motive force that causes a flow of protons from the intermembrane space into the cytoplasm via ATP synthase.

desired goal, with the rate of incident in 2021 falling only by 11% and mortality falling by 9.2% [2].

An effective strategy to arrest the growth of actively replicating and dormant *M. tuberculosis* might consist in targeting components of the oxidative phosphorylation pathway (Fig. 1) [3]. The chain is comprised of several plasma membrane proteins including the cytochrome bc_1, which is part of the cytochrome bc_1-aa_3 super complex [4]. The latter is involved in electron transfer processes, *e.g.*, the oxidation of ubihydroquinone and reduction of cytochrome in bacterial oxidative phosphorylation chains [5] and is a potential TB drug target that can be inhibited by different chemotypes [6]. The menaquinol-binding (Qp) site of the QcrB subunit of cytochrome bc_1 seems to be the preferred target of the cytochrome bc_1-aa_3 inhibitors reported to date including, but not limited to, 2-(quinolin-4-yloxy)acetamides (QOAs) [7–12], lansoprazole [13], imidazo[4,5-*c*]pyridine [14] and imidazo[1,2-*a*]pyridines amides (IPAs) [15], e.g., Q203 [16,17] and ND-008454 [18], morpholino thiophenes [19], anilinyl-analogues of phenoxyalkylbenzimidazoles (PABs) [20] and triazolopyrimidines, such as TPN-0006239 [21] (Fig. 2).

Q203 has recently completed phase II clinical trials [22] for TB treatment (https://clinicaltrials.gov/ct2/show/NCT03563599) and was found to be effective against MDR and XDR TB by targeting cytochrome bc_1. Mutations T313I or T313A (e.g., mutation of T313 to isoleucine and alanine, T313I and T313A, respectively) within QcrB were found to be cause of resistance against Q203 [23], whereas a L176P mutation was responsible for the resistance to lansoprazole [13].

The remarkable anti-tubercular activity of previously reported 4-substituted oxy- and thio-quinolines, such as 4-((4-(tert-butyl)benzyl) thio)-6-methoxy-2-methylquinoline (**1**, also referred to as **5***a* in this study), and their facile synthesis, prompted us to further investigate the mechanism of action of this class of compounds [8,24]. Given the structural analogy of 4-thio-quinolines and their oxy- and sulfoxy- analogues with the QOA scaffolds, we postulated, along with other research groups, [8] that 4-substituted quinoline-compounds might exert their anti-tubercular activity by targeting the QcrB unit of the cytochrome bc_1 oxidoreductase complex.

Here, a library of 4-substituted sulfoxide-, oxy- and thio-quinoline analogues was synthesised and evaluated for their ability to inhibit the growth of *M. tuberculosis* wild-type and T313I mutant strains. The library included both previously reported oxy- and thio-quinolines [8,24] and novel derivatives containing an expanded range of aryl moieties, e.g., pyridine, quinoline, indole and *meta*-chloro substituted methoxybenzyl rings, attached to the quinoline unit of the final products. Moreover, sulfoxy- and oxy-quinoline derivatives were tested for antitubercular activity for the first time. In general, QcrB mutant strains were resistant to the 4-substituted thioquinoline compounds, which induced depletion of intracellular ATP, thus showing evidence of targeting the cytochrome bc_1 oxidase complex. On the other hand, 4-oxyquinoline and sulfoxy-quinoline derivatives were less active against *M. tuberculosis* H37Rv compared to the thio-quinoline class. However, two novel derivatives, **4***i* and **5** *g*, had greater growth inhibitory properties against the QcrB mutant strains, with the 4-quinolinyl-oxy-quinoline compound **4***i* showing 6.5-fold higher selectivity for the QcrB T313I mutant strain compared to the wild-type, indicating QcrB as the cellular target.

2. Results and discussion

2.1. 4-Aryl-substituted-thioquinolines disrupt energy metabolism in *M. Tuberculosis*

To test our hypothesis that aryl thiol ether quinolines target the *M. tuberculosis* H37Rv bc_1 complex, we synthesised previously reported anti-tubercular agent **1** (**5***a*) [24]. Compound **1** (**5***a*) was evaluated for cytotoxicity in HepG2 cells and growth inhibitory activity against mutant strains expressing $QcrB_{T313I}$ or $QcrB_{M342T}$. Analogue **1** (**5***a*) was

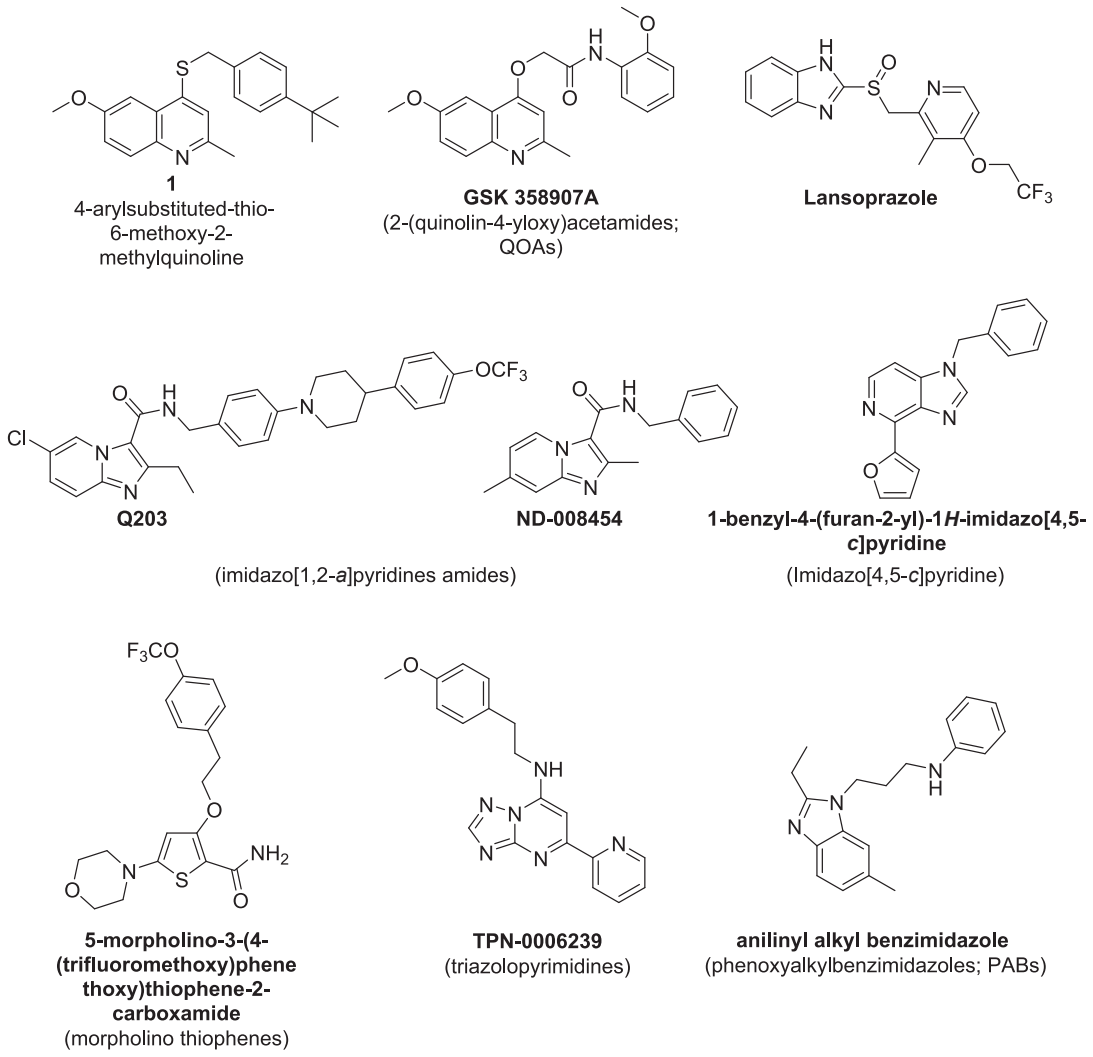

Fig. 2. Structures of lead compound **1**, which emerged from a GSK phenotypic screening campaign, and chemical scaffolds targeting *M. tuberculosis* QcrB unit of the menaquinol cytochrome *c* oxidoreductase (bc_1 complex), which is part of the bc_1-aa_3-type cytochrome oxidase complex. Scaffolds include 2-(quinolin-4-yloxy) acetamides (QOAs), lansoprazole, imidazo[4,5-*c*]pyridine and imidazo[1,2-]pyridines amides (IPAs), anilinyl-analogues of phenoxyalkylbenzimidazoles (PABs) and triazolopyrimidines.

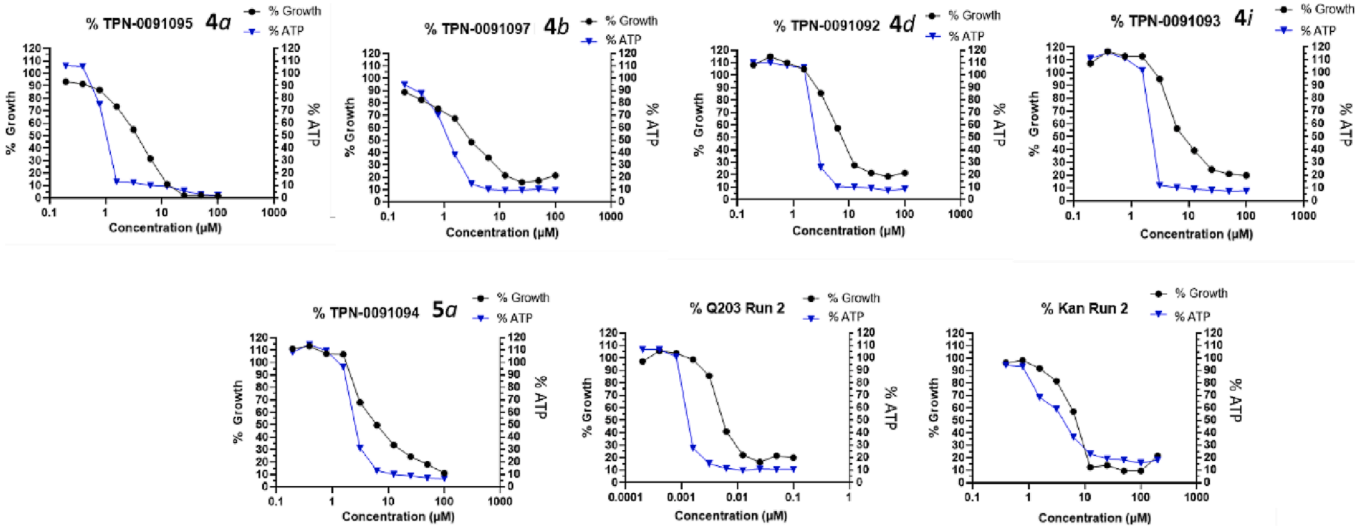

Fig. 3. Compounds **4***a*, **4***b*, **4***d*, **4***i* and **5***a* induced depletion of intracellular ATP levels. ATP concentrations were measured using the BacTiter Glo assay kit in *M. tuberculosis* after incubation with the quinoline compounds for 24 h.

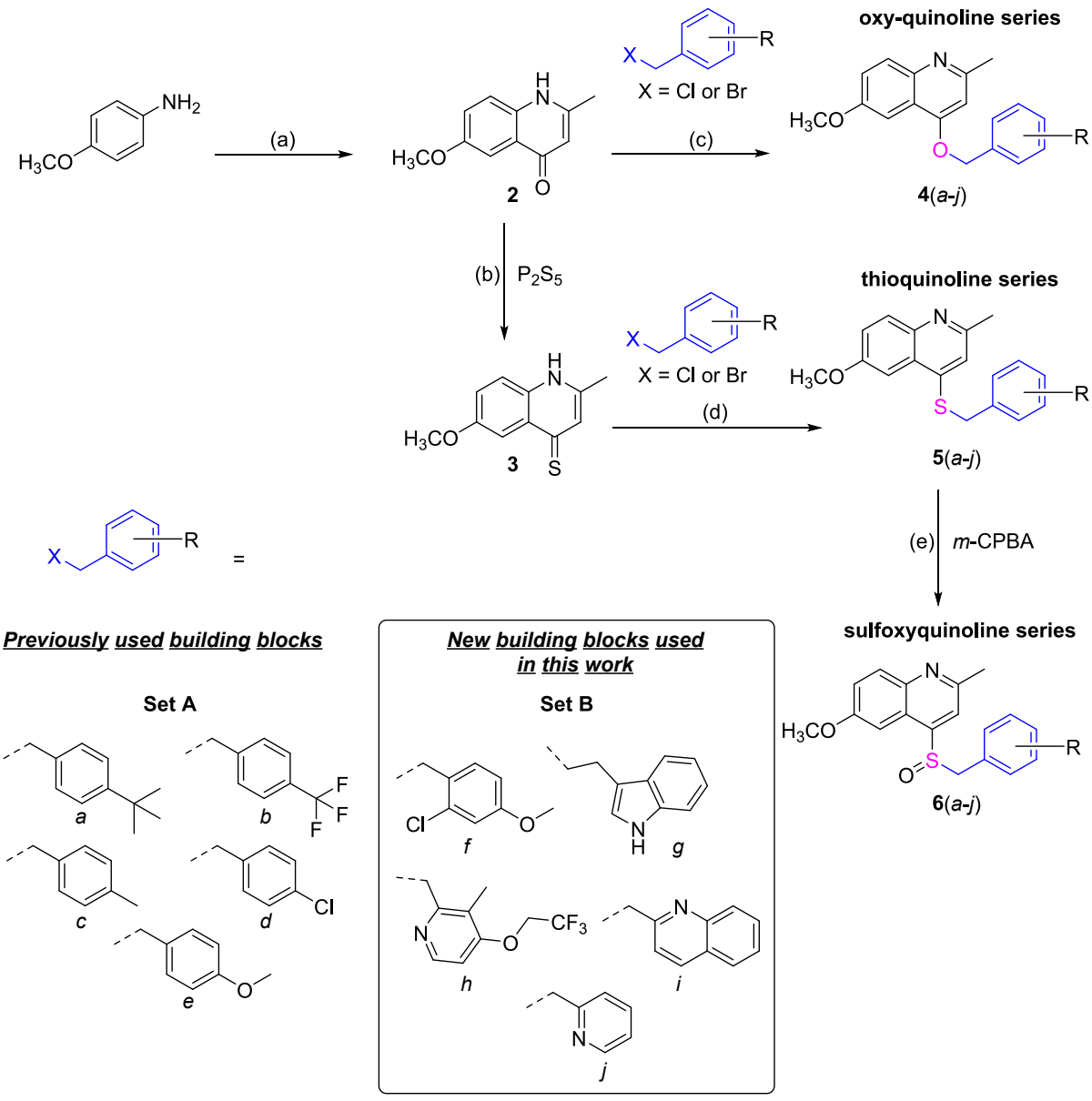

Scheme 1. Reagents and reaction conditions. (a) *Part 1*: ethyl acetoacetate, acetic acid, *p*-anisidine, anhydrous toluene, 80 °C Dean-Stark apparatus, 2 h; *Part 2*: Phenyl ether-biphenyl eutectic, 245 °C at reflux, 1 h; (b) Lawesson's reagent, anhydrous toluene, 80 °C, 4 h; (c) aryl alkyl halide, K_2CO_3, anhydrous DMF, r.t., 2.5–72 h; (d) aryl alkyl halide 2 M NaOH, anhydrous methanol, 0 °C to r.t., 2 h − 9 days; (e) *m*-CPBA, anhydrous DCM, −25 °C to r.t., 24 h − 7 days.

also tested for its ability to deplete intracellular ATP levels under aerobic conditions in *M. tuberculosis* (Fig. 3). In this study, we used previously reported resistant strains T313I and M342T [18,20] that were derived from the parental strain *M. tuberculosis* H37Rv-LP (ATCC 25618) carrying single-nucleotide polymorphisms of the *qcr*B gene, which encodes a subunit of the menaquinol cytochrome *c* oxidoreductase (bc_1) complex.

A 22-fold shift in growth inhibition was observed for **1** (**5***a*) in the strain with $QcrB_{M342T}$ (MIC_{90} = 2.6 μM) and a 4-fold shift in the strain with $QcrB_{T313I}$ (MIC_{90} = 0.47 μM) compared to wild-type *M. tuberculosis* H37Rv (MIC_{90} = 0.12 μM), thus confirming the activity of this thioquinoline was targeting the QcrB subunit. Compound **1** (**5***a*) showed mild cytotoxicity in HepG2 cells cultured in both galactose and glucose media ($IC_{50\ Glu}$ = 48 μM/$IC_{50\ Gal}$ = 34 μM; Glu/Gal Ratio = 1.4).

Compounds that inhibit cytochrome bc_1 oxidase have previously been shown to deplete intracellular ATP levels in aerobic cells [11]. As can be noted in the graph of Fig. 3, there was a clear depletion of ATP in *M. tuberculosis* cells in response to compound **1** (**5***a*) treatment. Thioquinoline **1** (**5***a*) was able to reduce ATP levels within 24 h of exposure under aerobic conditions. Q203, a known cytochrome bc_1 inhibitor, was used as the control.

After establishing that 4-substituted thio-quinolines targeted respiratory processes in *M. tuberculosis*, we set out to prepare a library of compound **1** analogues to gather structural activity relationship data. In addition to novel quinoline-based probes, the library included a number of previously reported derivatives, which were synthesised and screened to gather further information about the ability of variously substituted quinoline-including compounds to target respiratory processes in *M. tuberculosis* strains. The probes were tested against strains carrying the QcrB mutation at T313I. This is one the most common mutations that causes resistance to inhibitors [21].

2.2. Synthesis of quinoline-compound analogues

The structure of 6-methoxy-2-methylquinolin-4-ol (**2**) was synthesised from ethyl acetoacetate and *p*-anisidine using the Conrad-

Table 1
Inhibitory concentrations against wild-type and QcrB T313I *M. tuberculosis* strains[a] and HepG2 (IC_{50})[b] toxicity of selected new 4-substituted quinoline analogues.

Compound	*M. tuberculosis*				HepG2	Selectivity Index (SI)[c]
	H37Rv (Wild-type)		QcrB T313I			
	IC_{90} (μM)	IC_{50} (μM)	IC_{90} (μM)	IC_{50} (μM)	IC_{50} (μM)	
4*f*	>100	>100	ND	ND	30	ND
4*h*	77	37	53	32	4.9	0.1
4*i*	47	7.3	7.3	4.7	ND	ND
5*f*	0.78	0.21	ND	ND	13	62
5*g*	43	11	20	5.1	4.3	0.4
5*h*	24	11	18	8.5	4.0	0.4
5*i*	0.17	0.042	ND	ND	33	786
5*j*	2.7	0.6	1.5	0.69	72	120
6*b*	0.63	0.14	ND	ND	6.8	49
6*d*	0.7	0.26	ND	ND	7.7	30
6*e*	0.83	0.093	ND	ND	2.8	30
Rifampicin	0.0087	0.0044	0.0041	0.0019	ND	ND

[a] Inhibitory concentrations (ICs) were determined after 5-day incubation period. IC_{90} and IC_{50} are the compound concentrations that would inhibit the growth of 90% and 50%, respectively, of the tested bacterial isolates. The parental strain is *M. tuberculosis* H37Rv-LP (ATCC 25618). [b]IC_{50} is the concentration required to reduce HepG2 cell number by 50% and was determined after 3 days of exposure to compounds [c]SI is the ratio between GIC_{50} and the $IC_{90\ H37Rv}$. ND = Not Determined. [d]Compounds' structures and antimycobacterial activity previously reported [8,24].

Limpach condensation reaction [9,24] (Scheme 1). Sulfur-containing 6-methoxy-2-methylquinolin-4-thiol analogue **3** was obtained by treating **2** with Lawesson's reagent. Quinoline scaffolds **2** and **3** were subsequently coupled to aryl alkyl halide building blocks (Set A and Set B) to give oxyquinoline **4**(*a-j*) and thioquinoline **5**(*a-j*) compounds. The sulfoxide-quinoline compounds series **6**(*a-j*) was obtained by treating thioquinoline analogues **5**(*a-j*) with *m*-CPBA. The use of Set A aryl/hetaryl alkyl moieties led to previously reported analogues **4**(*a-e*), **5***a* (*i.e.*, compound **1**), **5***b-e* and **6***a* [24], whereas the use of Set B (and part of Set A) building blocks allowed for the synthesis of 19 novel quinoline derivatives **4***f-j*, **5***f-j* and **6***b-j*.

2.3. Anti-mycobacterial screening

Determination of activity (IC_{50} and IC_{90}) against H37Rv wild-type *M. tuberculosis* strain confirmed the potency of previously reported thioquinolines **5***b*, **5***c*, **5***d*, **5***e* [24] with IC_{90} values ranging from 0.025 – 0.63 μM (Table S2). New 4-thioquinoline analogues **5***f* (MIC_{90} = 0.78 μM; MIC_{50} = 0.21 μM), **5***i* (MIC_{90} = 0.17 μM; MIC_{50} = 0.042 μM), and pyridine-containing **5***j* (MIC_{90} = 2.7 μM; MIC_{50} = 0.6 μM) were found to be effective *M. tuberculosis* growth inhibitors, whereas indole- (**5** *g*), and trifluoro-ethoxy pyridine- (**5** *h*) including analogues were mildly active (Table 1).

Generally, oxyquinoline derivatives exhibited moderate activity against the H37Rv wild-type strain. For example, **4***a* was found to be the most potent of this series (MIC_{90} = 1.7 μM), whereas **4***d* was > 100-fold less active than its thio-quinoline counterpart **5***d* (Table S2).

The presence of the sulfoxide group in the quinoline scaffold structure restored the anti-tubercular activity of the compounds. Novel sulfoxide containing compounds **6***b*, **6***d* and **6***e* effectively inhibited the growth of *M. tuberculosis* H37Rv with IC_{90} values ranging between 0.2 and 0.83 μM and IC_{50}.values ranging from 0.043 to 0.26 μM.

IC screening of the compounds against QcrB resistant mutant T313I revealed a shift in activity for selected 4-arylalkyl substituted thio- and oxy-quinolines, thus confirming our hypothesis that this class of compounds targeted mitochondrial respiration enzymes in *M. tuberculosis*. It was noted that there were differences between IC_{50} and IC_{90} values in the growth inhibitory curves of QcrB mutants. This can be partially attributed to the fact that the T313I strain grows more slowly than the wild-type *M. tuberculosis* strain. As a result, IC_{50} instead of IC_{90} values were mainly used to assess the compounds activity against QcrB mutants. A decrease in growth inhibitory activity against the mutant strain compared to wild-type H37Rv was observed for both thioquinoline, *i.e.*, **5***d* (42-fold) and **5***b* (3-fold), and to a lesser extent for oxyquinoline, *i.e.*, **4***a* (8-fold), **4***b* (10-fold) and **4***d* (5.9-fold), analogues (Table S2). The diminished activity of **5***b* and **5***d* in the QcrB mutants might be ascribable to reduced interactions between the *p*-chlorophenyl group of **5***d* or trifluoromethyl group of **5***b* with the mutated aminoacid residue at position 313 of the QcrB unit.

Table 2
Docking scores of selected 4-substituted thio-, oxy- and sulfoxy-quinolines against M. tuberculosis wild type (WT) and mutant (T313I) QcrB protein as targets. The average docking scores obtained by Autodock Vina were calculated from the top scores obtained for representative structures of five most populated clusters in each trajectory. The $Plants_{CHEMPLP}$ docking scores [25] were obtained by rescoring all poses obtained against the second clusters for of QcrB and difference was calculated between corresponding T313I and H37Rv WT poses.

Compounds	Average docking score (kcal/mol)		Docking score of most favourable poses (kcal/mol)		Difference of $Plants_{CHEMPLP}$ scores
	M. tuberculosis strains				
	H37Rv WT	T313I	H37Rv WT	T313I	T313I - H37Rv WT
4*d* (rm12)	−8.4	−8.8	−8.6	−9.1	−11.3
4*f* (rm10)	−8.5	−8.7	−8.8	−9.3	−10.5
4*h* (rm4)	−9.2	−9.2	−9.5	−9.8	−14.4
4*i* (rm14)	−9.5	−9.8	−9.7	−10.2	−4.4
5*a* (rm15)	−9	−9.4	−9.5	−9.7	−0.4
5*b* (rm19)	−9.4	−9.7	−9.7	−10.2	1.9
5*c* (rm7)	−8.6	−8.8	−8.9	−9.2	2.9
5*d* (rm11)	−8.4	−8.6	−8.7	−8.8	−1.7
5*g* (rm21)	−9.1	−9.3	−9.3	−9.8	−8.0
5*h* (rm9)	−8.5	−8.5	−8.8	−8.9	−5.9
5*i* (rm13)	−9.6	−9.8	−9.9	−10.2	−14.9
6*a* (rm15.1)	−9.1	−9.5	−9.5	−9.9	−0.4
6*b* (rm19.1)	−9.6	−9.9	−9.9	−10.3	−6.7
6*d* (rm11.1)	−8.6	−8.8	−8.8	−9.1	−12.4
6*e* (rm23.1)	−8.6	−8.5	−8.9	−8.7	−17.3
6*i* (rm13.1)	−9.6	−9.8	−10.1	−10	−6.4
Q203	−10.6	−11.1	−10.9	−11.9	−16.9

Interestingly, quinolin-2-yl–methyl–oxyquinoline **4***i* and (1*H*-indol-3-yl)ethyl)-thioquinoline **5** *g* were the only library members tested that exhibited 1.7-fold and 2.2-fold higher activity against QcrB T313I ($IC_{50\ QcrB\ T313I}$ = 4.7 and 5.1 μM, respectively) compared to the wild-type strain ($IC_{50\ H37Rv}$ = 7.3 and 11 μM, respectively), thus indicating affinity toward the target within the electron transport chain of *M. tuberculosis* mitochondria. If the IC_{90} values of **4***i* were used to compare the activity in wild-type vs mutated strains, the shift would be even more pronounced with a 6.5-fold decrease in activity against the wild-type (IC_{90} = 47 μM) compared to T313I mutant strain (IC_{90} = 7.3 μM).

Selected derivatives were screened for cytotoxicity in HepG2 cells and showed moderate to low toxicity. The new thioquinolines **5***i* and **5***j* were the least cytotoxic of the tested compounds with IC_{50} values of 33 and 72 μM, respectively, and favourable selectivity index (SI = ratio between $GIC_{50\ HepG2}$ and the $IC_{50\ H37Rv}$) values of 786 and 120, respectively. Novel sulfoxy-quinoline analogue **6***b*, which contained a trifluoromethyl-phenyl residue, showed an $IC_{50\ HepG2}$ value of 6.8 μM and had a SI of 49, whereas **6***e* exhibited an IC_{50} value of 0.093 against H37Rv and a SI of 30.

2.4. ATP depletion

Measurement of ATP production in mycobacteria can provide

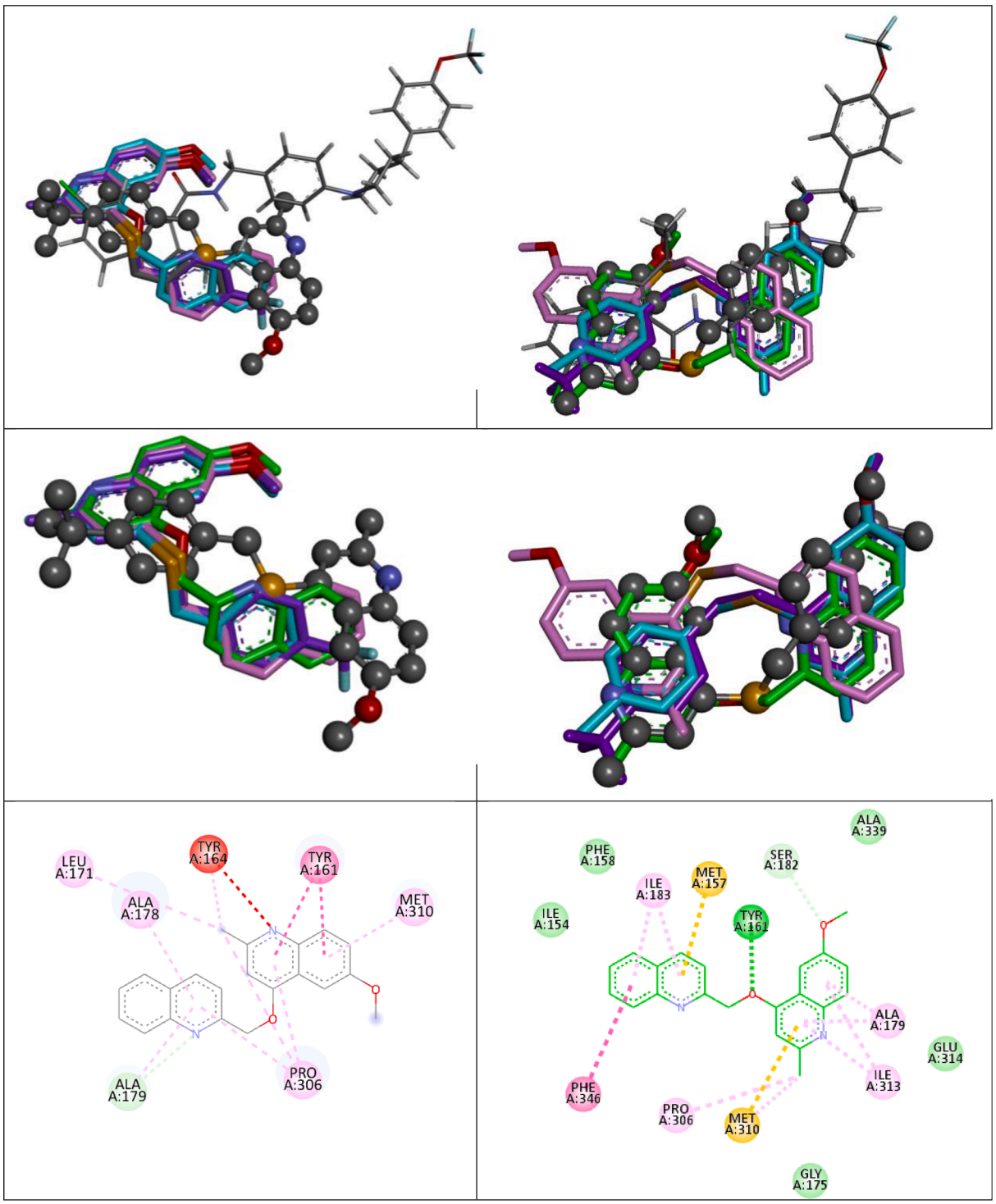

Fig. 4. Overlay of selected active molecules and Q203 in the binding sites of the wt (left) and T313 mutant (right) QcrB. Q203 is shown in a thin stick representation and **5***b* is represented as a ball and stick, both having carbon atoms coloured in grey. The active analogues are shown in a thick stick representation with carbon atoms coloured as followed: **4***i* – green carbons; **5***d* – cyan carbons; **5***i* – pink carbons and **5***b* – purple carbons. The 2D protein ligand interactions plots are shown for **4***i* in the binding sites of the wt (left) and T313 mutant (right) strains.

additional information on compounds' ability to inhibit aerobic respiration processes (e.g., electron transport chain and ATP synthase). Inhibition of cytochrome bc_1 leads to reduced movement of protons across the membrane, thus resulting in less build-up of proton ions outside of the mitochondrial membrane. A low proton gradient results in a decrease of ATP production, as there are less proton ions passing through the ATP synthase, which in turn cannot catalyse the conversion of ADP to ATP. Compounds **4***a*, **4***b*, **4***d*, **4***i* and **5***a* were incubated with *M. tuberculosis* for 24 h and ATP levels were determined using the BacTiter-Glo assay kit (Promega). Growth was measured by optical density at 590 nm (OD_{590}). All of the tested compounds, including positive control Q203, were able to deplete ATP production in a dose-dependent manner at concentrations that did not inhibit *M. tuberculosis* growth (*i.e.*, lower than IC_{50} growth inhibition values) (Fig. 3). Kanamycin, which does not target electron chain transport mechanisms, did not cause ATP depletion. This constitutes further

evidence that thioquinoline and oxyquinoline probes mode of action may reside in their ability to target cytochrome bc_1 complex and disrupt electron transfer in the respiratory chain of tubercle bacilli mitochondria.

2.5. Molecular modelling

The molecular docking results reported in Table 2 revealed that on average ligands were predicted to bind tighter into the binding pocket of the mutant QcrB protein compared to that of the WT protein. Although the analogues are closer aligned with the inactive conformation of Q203 in the binding site of the $QcrB_{T313I}$ *M. tuberculosis* mutant, they have different binding modes. It can also be noted that quinolin-2-yl–methyl–containing derivatives **4*i*** (oxy-quinoline series), **5*i*** (thioquinoline series) and **6*i*** (sulfoxiquinoline series) were predicted to bind to the T313I mutated protein with higher affinity compared to other library members. These results might in part explain the 6.5-fold higher antitubercular activity of **4*i*** against QcrB T313I compared to the wild-type strain. As can be seen in Fig. 4, 4**i** has an increased number of interactions with amino acid residues at the QcrB T313I binding site. These include contacts of the **4*i*** oxyquinoline core with mutated isoleucine 313, hydrogen bonding of tyrosine 161 with the oxygen atom of the compound's methyl-oxy-bridge, van der Waals interactions between the phenylalanine 346 benzyl group and the quinolin-2-yl northern aryl moiety of the ligand. The full atomistic molecular dynamics simulation of mutated QcrB – **4*i*** complex has confirmed that the key interactions between the ligand and hydrophobic residues (A179, I183 and I313) were preserved throughout the 100 ns trajectory. This suggests that the hydrophobic pocket of T313I mutant (Fig. S1) could be the target site for these novel analogues and will be subject of further studies.

3. Conclusions

The facility to access the 4-substituted quinoline framework and the remarkable anti-tubercular activity of previously reported derivatives prompted us to further investigate this scaffold by expanding the array of aryl-group positioned at the C-4 position of the quinoline unit and evaluating the ability of thio-, oxy- and sulfoxide-derivatives to inhibit the cytochrome oxidase complex. It was found that the oxyquinoline series had moderate activity against both H37Rv and QcrB T313I mutant strains of *M. tuberculosis* used in this study, whereas novel sulfoxide-bearing derivatives **6*b***, **6*d*** and **6*e***, and thioquinolines **5*f***, **5*i*** inhibited the growth of the Koch bacillus in the 42–260 nM range, with new compound **5*i*** being active at low nanomolar levels ($IC_{50\ H37Rv} = 42$ nM).

A shift in anti-tubercular activity against QcrB resistant mutant T313I for **4*a,*** **4*d***, **5*a***, **5*b*** and **5*d*** confirmed that 4-arylalkyl substituted thio- and oxy-quinolines targeted mitochondrial respiration enzymes in *M. tuberculosis*. Measurement of depletion of intracellular ATP levels in *M. tuberculosis* further corroborated these results, as thio- and oxy-quinolines induced ATP depletion.

Remarkably, novel quinolin-2-yl–methyl–oxyquinoline **4*i*** showed higher activity against QcrB T313I compared to the wild-type strain. Further, **4*i*** induced depletion of intracellular ATP levels and was predicted to bind to the T313I mutated protein with higher affinity compared to other analogues. Moreover, another novel thioquinoline compound, **5*g***, was also found to have higher activity against QcrB T313I. This is an interesting finding related to the potential ability of bulky aryl-moieties, *i.e.,* quinolyl- and indolyl moieties, attached to the oxy- and thio-quinoline rings to modulate interactions with QcrB sites. It is also worth considering that bioisosteric exchange between oxygen and sulfur, coupled with insertions of bulky northern aryl unit in the quinoline frames, might maintain activity and interactions with the molecular target in the mutated *M. tuberculosis* strain.

Taken together, these findings suggests that quinoline derivatives might serve as a scaffold to develop new QcrB targeted probes and improve the level of efficacy previously observed for this class of compounds. Further, the novel quinolinic probes described here can be used as tool compounds to study oxidative phosphorylation processes in mycobacteria.

Declaration of Competing Interest

The authors declare that they have no known competing financial interests or personal relationships that could have appeared to influence the work reported in this paper.

Data availability

Data will be made available on request.

Acknowledgement

We thank Lauren Ames and Quan Pham for technical assistance.

Appendix A. Supplementary data

Supplementary data to this article can be found online at https://doi.org/10.1016/j.bioorg.2023.106659.

References

[1] Organization ed.,, World Health Organization, 2020. Global tuberculosis report 2021.
[2] C. Jeremiah, E. Petersen, R. Nantanda, B.N. Mungai, G.B. Migliori, F. Amanullah, P. Lungu, F. Ntoumi, N. Kumarasamy, M. Maeurer, A. Zumla, The WHO Global Tuberculosis 2021 Report–not so good news and turning the tide back to End TB, Int. J. Infect. Dis. (2022).
[3] W.D. Hong, P.D. Gibbons, S.C. Leung, R. Amewu, P.A. Stocks, A. Stachulski, P. Horta, M.L.S. Cristiano, A.E. Shone, D. Moss, A. Ardrey, R. Sharma, A. J. Warman, P.T.P. Bedingfield, N.E. Fisher, G. Aljayyoussi, S. Mead, M. Caws, N. G. Berry, S.A. Ward, G.A. Biagini, P.M. O'Neill, G.L. Nixon, Rational design, synthesis, and biological evaluation of heterocyclic quinolones targeting the respiratory chain of Mycobacterium tuberculosis, J. Med. Chem. 60 (9) (2017) 3703–3726.
[4] K. Pethe, P. Bifani, J. Jang, S. Kang, S. Park, S. Ahn, J. Jiricek, J. Jung, H.K. Jeon, J. Cechetto, T. Christophe, H. Lee, M. Kempf, M. Jackson, A.J. Lenaerts, H.a. Pham, V. Jones, M.J. Seo, Y.M. Kim, M. Seo, J.J. Seo, D. Park, Y. Ko, I. Choi, R. Kim, S. Y. Kim, SeungBin Lim, S.-A. Yim, J. Nam, H. Kang, H. Kwon, C.-T. Oh, Y. Cho, Y. Jang, J. Kim, A. Chua, B.H. Tan, M.B. Nanjundappa, S.P.S. Rao, W.S. Barnes, R. Wintjens, J.R. Walker, S. Alonso, S. Lee, J. Kim, S. Oh, T. Oh, U. Nehrbass, S.-J. Han, Z. No, J. Lee, P. Brodin, S.-N. Cho, K. Nam, J. Kim, Discovery of Q203, a potent clinical candidate for the treatment of tuberculosis, Nat. Med. 19 (9) (2013) 1157–1160.
[5] D.i. Xia, L. Esser, W.-K. Tang, F. Zhou, Y. Zhou, L. Yu, C.-A. Yu, Structural analysis of cytochrome bc1 complexes: Implications to the mechanism of function, Biochimica et Biophysica Acta (BBA) - Bioenergetics 1827 (11-12) (2013) 1278–1294.
[6] Huszár S, Chibale K, Singh V. The quest for the holy grail: new antitubercular chemical entities, targets and strategies. *Drug Discovery Today*. **2020**, *25*(4), 772-80; Bahuguna A, Rawat S, Rawat DS. QcrB in Mycobacterium tuberculosis: The new drug target of antitubercular agents. *Medicinal Research Reviews*. **2021**, *41*(4), 2565-2581.
[7] K. Pissinate, A.D. Villela, V. Rodrigues-Junior, B.C. Giacobbo, E.S. Grams, B. L. Abbadi, R.V. Trindade, L. Roesler Nery, C.D. Bonan, D.F. Back, M.M. Campos, 2-(Quinolin-4-yloxy) acetamides are active against drug-susceptible and drug-resistant Mycobacterium tuberculosis strains, ACS Med. Chem. Lett. 7 (3) (2016) 235–239.
[8] A.F. Borsoi, J.D. Paz, B.L. Abbadi, F.S. Macchi, N. Sperotto, K. Pissinate, R. S. Rambo, A.S. Ramos, D. Machado, M. Viveiros, C.V. Bizarro, Design, synthesis, and evaluation of new 2-(quinoline-4-yloxy) acetamide-based antituberculosis agents, Eur. J. Med. Chem. 192 (2020), 112179.
[9] E. Pitta, M.K. Rogacki, O. Balabon, S. Huss, F. Cunningham, E.M. Lopez-Roman, J. Joossens, K. Augustyns, L. Ballell, R.H. Bates, P. Van der Veken, Searching for new leads for tuberculosis: design, synthesis, and biological evaluation of novel 2-quinolin-4-yloxyacetamides, J. Med. Chem. 59 (14) (2016) 6709–6728.
[10] L. Ballell, R.H. Bates, R.J. Young, D. Alvarez-Gomez, E. Alvarez-Ruiz, V. Barroso, D. Blanco, B. Crespo, J. Escribano, R. González, S. Lozano, Fueling open-source drug discovery: 177 small-molecule leads against tuberculosis, ChemMedChem. 8 (2) (2013) 313–321.
[11] N. Phummarin, H.I. Boshoff, P.S. Tsang, J. Dalton, S. Wiles, C.E. Barry 3rd, B. R. Copp, SAR and identification of 2-(quinolin-4-yloxy) acetamides as Mycobacterium tuberculosis cytochrome bc 1 inhibitors, MedChemComm 7 (11) (2016) 2122–2127.

[12] F.T. Subtil, A.D. Villela, B.L. Abbadi, V.S. Rodrigues-Junior, C.V. Bizarro, L.F.S. M. Timmers, O.N. De Souza, K. Pissinate, P. Machado, A. López-Gavín, G. Tudó, Activity of 2-(quinolin-4-yloxy) acetamides in Mycobacterium tuberculosis clinical isolates and identification of their molecular target by whole-genome sequencing, Int. J. Antimicrob. Agents 51 (3) (2018) 378–384.
[13] J. Rybniker, A. Vocat, C. Sala, P. Busso, F. Pojer, A. Benjak, S.T. Cole, Lansoprazole is an antituberculous prodrug targeting cytochrome bc1, Nat. Commun. 6 (1) (2015) 1–8.
[14] K. Arora, B. Ochoa-Montaño, P.S. Tsang, T.L. Blundell, S.S. Dawes, V. Mizrahi, T. Bayliss, C.J. Mackenzie, L.A. Cleghorn, P.C. Ray, P.G. Wyatt, Respiratory flexibility in response to inhibition of cytochrome C oxidase in Mycobacterium tuberculosis, Antimicrob. Agents Chemother. 58 (11) (2014) 6962–6965.
[15] K.A. Abrahams, J.A. Cox, V.L. Spivey, N.J. Loman, M.J. Pallen, C. Constantinidou, R. Fernández, C. Alemparte, M.J. Remuiñán, D. Barros, L. Ballell, G.S. Besra, Identification of novel imidazo[1,2-a]pyridine inhibitors targeting M. tuberculosis QcrB, PLoS One 7 (12) (2012) e52951.
[16] V.R. de Jager, R. Dawson, C. van Niekerk, J. Hutchings, J. Kim, N. Vanker, L. van der Merwe, J. Choi, K. Nam, A.H. Diacon, Telacebec (Q203), a new antituberculosis agent, N. Engl. J. Med. 382 (2020) 1280–1281.
[17] S. Zhou, W. Wang, X. Zhou, Y. Zhang, Y. Lai, Y. Tang, J. Xu, D. Li, J. Lin, X. Yang, T. Ran, Structure of Mycobacterium tuberculosis cytochrome bcc in complex with Q203 and TB47, two anti-TB drug candidates, Elife 10 (2021) e69418.
[18] T. O'Malley, T. Alling, J.V. Early, H.A. Wescott, A. Kumar, G.C. Moraski, M. J. Miller, T. Masquelin, P.A. Hipskind, T. Parish, Imidazopyridine compounds inhibit mycobacterial growth by depleting ATP levels, Antimicrob. Agents Chemother. 62 (6) (2018) e02439–e02517.
[19] L.A. Cleghorn, P.C. Ray, J. Odingo, A. Kumar, H. Wescott, A. Korkegian, T. Masquelin, A. Lopez Moure, C. Wilson, S. Davis, M. Huggett, Identification of morpholino thiophenes as novel Mycobacterium tuberculosis inhibitors, targeting QcrB, J. Med. Chem. 61 (15) (2018) 6592–6608.
[20] N.S. Chandrasekera, B.J. Berube, G. Shetye, S. Chettiar, T. O'Malley, A. Manning, L. Flint, D. Awasthi, T.R. Ioerger, J. Sacchettini, T. Masquelin, Improved phenoxyalkylbenzimidazoles with activity against Mycobacterium tuberculosis appear to target QcrB, ACS Infect. Dis. 3 (12) (2017) 898–916.
[21] C. Shelton, M. McNeil, R. Allen, L. Flint, D. Russell, B. Berube, A. Korkegian, Y. Ovechkina, T. Parish, Triazolopyrimidines target aerobic respiration in Mycobacterium tuberculosis, Antimicrob. Agents Chemother. 66 (4) (2022) e02041–e02121.
[22] B.S. Lee, E. Sviriaeva, K. Pethe, Targeting the cytochrome oxidases for drug development in mycobacteria, Prog. Biophys. Mol. Biol. 152 (2020) 45–54.
[23] L. Bown, S.K. Srivastava, B.M. Piercey, C.K. McIsaac, K. Tahlan, Mycobacterial membrane proteins QcrB and AtpE: roles in energetics, antibiotic targets, and associated mechanisms of resistance, J. Membr. Biol. 251 (1) (2018) 105–117.
[24] J. Escribano, C. Rivero-Hernández, H. Rivera, D. Barros, J. Castro-Pichel, E. Pérez-Herrán, A. Mendoza-Losana, Í. Angulo-Barturen, S. Ferrer-Bazaga, E. Jiménez-Navarro, L. Ballell, 4-Substituted thioquinolines and thiazoloquinolines: potent, selective, and tween-80 in vitro dependent families of antitubercular agents with moderate in vivo activity, ChemMedChem 6 (12) (2011) 2252–2263.
[25] O. Korb, T. Stutzle, T.E. Exner, Empirical scoring functions for advanced protein–ligand docking with PLANTS, J. Chem. Inf. Model. 49 (1) (2009) 84–96.